Monitoring scoliosis progression

Dewi, Dyah Ekashanti Octorina

Chapter 8

An Improved Olympic Hole-Filling Method for Ultrasound Volume Reconstruction of Human Spine

Published in International Journal of E-Health and Medical Communications
Vol. 1(3), pp. 30-42, July-September 2010

Abstract

Hole-filling in ultrasound volume reconstruction using freehand three-dimensional ultrasound (3DUS) is aimed to estimate the values for empty voxels from the unallocated voxels in the Bin-filling process due to inadequate sampling in the acquisition process. Olympic operator, as one of neighbourhood averaging filter, can be used to estimate the empty voxel. However, this method needs improvement to generate a closer estimation of the empty voxels.

In this paper, we propose an improved Olympic operator for the Hole-filling algorithm, and we also apply it to generate the volume in our 3D ultrasound reconstruction of the spine. First, the ultrasound frames and position information are compounded into a 3D volume using the Bin-filling method. Then, the Hole-filling method is used to repair gaps in the volume. The conventional Olympic operator defines the empty voxels by sorting the neighbouring voxels, removing the n% of the upper and lower values, and averaging them to attain the value to fill the empty voxels. The empty voxel estimation can be improved by thresholding the range width of its neighbouring voxels and adjusting it to the average values.

The method is tested on a hole-manipulated volume derived from a cropped 3D ultrasound volume of a part of the spine. Our MAE calculation on the proposed technique shows improved result compared to all tested existing methods.

Keywords

Hole-filling, improved Olympic operator, 3D reconstruction, freehand, ultrasound, spine.

8.1. Introduction

The use of three-dimensional ultrasound (3DUS) imaging in clinical applications has contributed to more extensive information for medical diagnoses. Significant improvements in the generation of structural volumetric representation enable better visualization and more accurate measurement and analysis [1-5]. One of the advanced developments is the generation of 3DUS imaging out of two-dimensional ultrasound (2DUS) system. In this regard, this 3DUS system employs mechanical or freehand scanning techniques [1;6;7]. The mechanical sweeps the region of interest by mounting the probe to a stepper motor to move the probe in a predefined manner where the relative position and angulation of each frame can be determined precisely. In contrast to the mechanical system, the freehand scanning acquires the region of interests by mounting a position tracking system to the probe. In this system, the scanning geometry is not predetermined [1;2;8;9]. However, both have their own advantages and drawbacks.

In the evaluation of the spine, ultrasound imaging has been proven to capture spinal features from the reflection of the ultrasound signal [10-12]. In the study of Suzuki [10], ultrasound is capable of outlining the spinous process and the laminae to measure axial rotation of the vertebrae. This method, however, only applies 2DUS scanned to the marked skin of the back. In fact, what can be seen in the ultrasound images is not the bony structure, but only the reflection of some parts of the bone surface as investigated by Brendel et al [11]. Purnama [12] has shown that the ultrasound signal reflects on the processi transversi and proved that such imaging system is an appropriate system to determine the shape of the human spine. Furthermore, to obtain the 3DUS volume of the spine, freehand scanning technique can be a good choice due to its flexibility to reach the whole spinal surface. However, imaging the spine using freehand 3DUS still suffers from an inadequate sampling process and speckle noise problems that may obscure the visibility of the spinal features causing inaccuracy in the extraction of the acquired vertebral features.

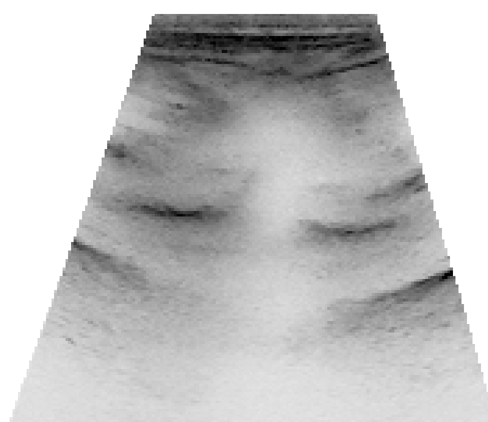

Figure. 8.1. The 2DUS frame of the thoracic spine

Figure. 8.1 illustrates one 2DUS frame from the thoracic vertebra part taken in axial plane using a linear probe with the frequency of 10 MHz, multiple focusing range of 3.5 to 5 cm, and imaging depth of 7 cm. From this example, the surface of the spinous process appears prominent as borderline between soft tissue structures. A dark shadow appears after the spinous process. Other features such as laminae, transverse processes, superior articular processes, ribs, and even pleura are also visible as reflected surfaces depending on the probe direction to certain locations of the vertebrae and their surrounding. The primary procedure in obtaining a 3DUS volume out of these 2DUS frames consists of two-step processes, acquisition of the ultrasound frame and position information, and reconstruction of the 3D volume [2]. The acquisition process grabs echo data based on the sweeping transducer arrays (an ultrasound probe) and information of a position-tracking system which determines the position of a sensor mounted on the ultrasound probe. This can be performed either from an integrated positional sensing device or from an external system. Since the spine has an elongated area of scanning and slanted parts in the thoracic and lumbar region, a flexible and large field of view (FOV) freehand 3DUS system is preferred to image the entire volume of the spine in any direction and movement [1;12;13]. The advantage of this system is a large adaptability for the probe movement in recording the position and orientation for 3D reconstruction with less distortions and errors.

The reconstruction process positions the acquired 2DUS frames into the 3DUS volume based on the correlated relative positions. This process depends on the acquisition of the 2D frames and the position of each frame. In general, the process can be simplified as follows. First, every acquired pixel in the 2DUS frame is extracted and scaled. Then, these pixels are combined with any offset values from one of the acquired positional parameters producing calibrated pixel values. For every calibrated pixel value, rotation matrices taken from the acquired positional parameter are applied to obtain a proper orientation and position of the pixels in the 2DUS frame into the matched part of the 3D volume. In this stage, the voxel value in each 3D volume position is updated by the pixel value of the associated 2DUS frame [14].

However, since the 3DUS volume is constructed from the 2D frames, variations in probe sweeping velocity and insufficient sampling rate could cause significant gaps and geometrical errors which obscure the 3D reconstruction process [1]. Various techniques have been proposed to obtain an optimal 3DUS volume reconstruction [2;15-21;21-24]. One of the most popular 3D reconstruction methods is Pixel Nearest Neighbour (PNN) [2;15;17;19;21;21;22].

In this paper, we propose an improved Hole-filling technique as alternative in the PNN algorithm based on an Olympic operation. The PNN algorithm is implemented in this study because of its simplicity and strength in resolving the computation time. To test the performance, the proposed method is applied to reconstruct a 3DUS volume of the spine and compared quantitatively with several existing methods [12];[19] using MAE (Mean Absolute Error).

8.2. Ultrasound Image Acquisition

The image acquisition using freehand 3DUS system requires synchronized position information on each captured 2DUS frame. In this study, a series of 2DUS frames were acquired using the GE LogiQ 9 ultrasound scanner (GE Healthcare, Chalfont St. Giles, UK) with a high resolution multi-frequency 2D probe (linear matrix array 10L with a frequency range of 6.3-10 MHz) allowing for a spatial resolution of 0.1-0.5 mm. We performed a B-mode scan with the frequency of 10 MHz using an SMP (Small Parts) ultrasound application with Musculoskeletal (MSK) exam study. The imaging depth was set at 7 cm with 3.5-5 cm of multiple focusing in a virtual convex feature to widen the FOV. According to the manufacturer, these settings are optimal for scanning the spinal features with this equipment.

The system is equipped with an electromagnetic position tracking system pcBIRD (Ascension Tech Corp, Burlington, VT, USA) supported with 3D FreeScan (Echotech 3D Imaging Systems GmbH, Germany). The electromagnetic position tracking system has a static position accuracy of 0.07" (1.8 mm) RMS and orientation accuracy of 0.5° RMS. It records spatial information for each captured 2D frames using a miniature magnetic field sensor within a transmitted pulsed magnetic field. In our study, the transmitter was located close to the subject with a maximum area range of 50 cm from the transmitter. The sensor was attached to the ultrasound probe bracket. The sensor contains 3 orthogonal coils to determine the magnetic field strength in 6 degree of freedom. The position and angulation in 3D space of the probe are determined by measuring the strength of the three components of the local magnetic field.

In this study, a healthy volunteer was positioned in prone position and the back of the volunteer was scanned in one column along the thoracolumbar area as seen in Figure. 7.6 of Chapter 7. A vacuum cushion system was applied in the frontal part of the body to fixate the position during scanning in lying down position on a bed. To avoid any misalignment due to physical movement of the subject, the subject was asked to hold his breath at full inspiration during scanning.

The scanning of the spine was performed in superior-inferior direction with the probe in axial plane. The probe sweeping was made as constant and dense as possible. This acquisition process resulted in sequential 2DUS frames with the synchronized position information from the position tracking system.

The imaging documentation of digital raw data in single 2D images with TIFF file format was collected using the existing general storage system. The associated positional information from the magnetic tracker recording, which consists of translation vector, rotation matrix, scaler value, and offset value in both acquisition and calibration modes, was used to calculate the transformation matrices. This transformation matrices are then utilized to obtain the voxel coordinates in the reconstructed 3D space and fill with the pixel coordinates in the 2DUS frame. It was located in the private extension tags of the each 2DUS frame file.

8.3. Ultrasound Volume Reconstruction

After collecting the 2DUS frames and the position information, the next step was reconstructing them into a 3D volume. The basic algorithm consists of two stages, Bin-filling and Hole-filling.

Bin-filling

This stage functions to map the 2D ultrasound frames into a 3D volume data set based on their corresponding positional information. In the freehand 3DUS imaging, the mapping of the coordinate system from a 2D frame to a 3D volume is defined by

$$u = Tw \tag{1}$$

where u is the transformed coordinate system in 3D space by transformation matrix T on the coordinate system w of the 2DUS frame.

The transformation matrix is obtained from the position information, where the relationship between the pixel coordinates in the original 2D frame (P), magnetic position sensor receiver (R), transmitter (T) and the voxel coordinates of the reconstructed 3D volume (C) can be formulated as

$$x_c = T_{CT} T_{TR} T_{RP} x_p \tag{2}$$

where x_c is the resulting voxel location in the reconstructed 3D volume C, and x_p is a pixel location in the 2DUS frame. T_{RP} denotes a transformation through the probe calibration from the acquired coordinates in the 2DUS frame P to the associated positional system in the magnetic position sensor receiver R, T_{TR} is the transformation taken directly from the positional system in the magnetic position sensor receiver R to the transmitter T, and T_{CT} is the positional alignment of the reconstructed 3D volume C with the transmitter T. The coordinate system used in this freehand 3DUS reconstruction system is described in Figure. 8.2.

In the Bin-filling process, every pixel in the 2D frame is translated, rotated, and scaled based on the transformation of the acquired position information to obtain the corresponding voxel in the 3D volume. When the voxel in the 3D space has not been occupied by any pixels from the 2D frame, the voxel value is then filled with the associated pixel value from the acquired 2D frame. For each pixel in the acquired 2DUS frame, the algorithm calculates the new voxel coordinate for the 3DUS space based on the transformation matrices from the associated position information, and fills the new voxel coordinate with the correlated pixel value.

However, due to the nature of freehand imaging system, it is highly possible that one voxel coordinate is filled with more than one pixel value from several intersecting 2D frames taken in different directions [22;25;26]. The challenge in this stage is solving a sampling problem in the determination of the final intensity of a voxel when pixels from several 2D frames occupy one voxel (known as spatial compounding). Previous studies [12;16;19;20;22;23] proposed on finding a minimum, maximum, median, most recent, average, or first value of the residing voxels [2]. Nonetheless, defining the best approach depends on the application and the characteristic of the object.

The bone surface reflections in the 3DUS volume have a higher intensity than the surrounding structures. Furthermore, such structure has a specific size and shape, and is located in a certain position in 3D space repetitively. However, some gaps due to missing voxels appear as small holes and blank lines in certain parts of the volume which may obscure the recognition of the reflected areas. In this regard, seeing that our application is specifically recognizing the reflection of the vertebral parts surface, taking the maximum value of the residing voxels is considered to be the best option.

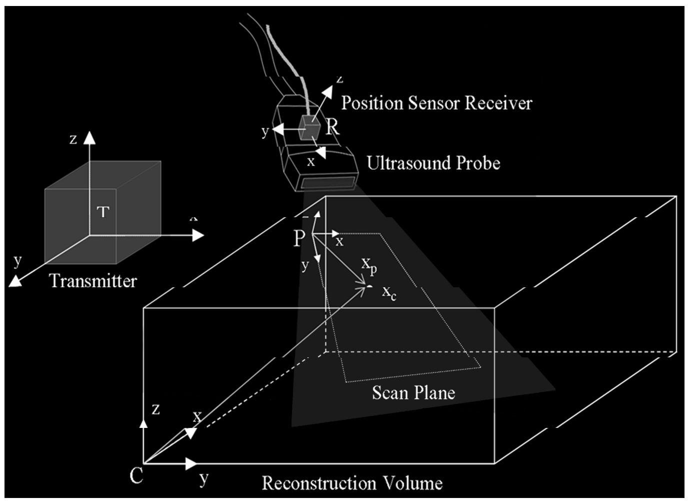

Figure. 8.2. Coordinate system in the 3DUS reconstruction using electromagnetic position tracking system. The coordinate systems applied in this system include the pixel coordinates of the 2DUS frame (P), magnetic position sensor receiver (R), transmitter (T), and the voxel coordinates of the reconstructed 3D volume (C)

Hole-filling

The Hole-filling process is accomplished when gaps occur in the voxel array due to inadequate sampling in the acquisition process. The aim of Hole-filling is to estimate the empty values based on its neighbouring voxels. Only when the frames are taken densely close, Hole-filling may not be needed [16].

In the PNN method, a variety of approaches have been developed previously. McCann [18] and Nelson et al [19] have suggested to average the empty voxels with the values from the local neighbours. Hottier and Collet Billon [17] have proposed to interpolate between the two closest non-empty voxels in the transverse direction. In the study of Purnama [12] in imaging the human spine, the use of the Olympic operation has been introduced. This method defines the empty voxels by sorting the neighbouring voxels, removing the *n*% of the upper and lower values, and averaging them to attain the final value for the empty voxels. Taking *n*=20 has given the most optimal result [12].

The main problem in the Hole filling algorithm is finding an optimal interpolation method to fill the gaps between frames in 3D volume without missing any information of interest or introducing any new noise. Moreover, the methods for filling the gaps, at some stages, need to be adapted based on the application and the specification of the reconstructed object.

8.4. Improved Olympic Hole Filling

A new Hole-filling technique to estimate the existing empty voxels, the improved Olympic operator, is proposed. The conventional Olympic operator [27] is a neighbourhood averaging filter which removes the *n%* of highest and lowest values in the kernel and replaces the centre value with the average of the remaining values.

The improvement is performed by employing the conventional Olympic operator, thresholding the range width of the remaining neighbouring empty voxels using the average of the range width of all existing empty voxels in the volume, and adjusting the weighting value that corresponds between the average and range width values to obtain the estimated empty voxel. The algorithm of the improved Olympic Hole-filling is explained in the following lines.

First, the 26 neighbouring voxels of the empty voxel with distance of r=1 voxel must be determined. This is obtained by taking connections from an empty voxel to all directions in the cubic neighbourhood as illustrated in Figure. 8.3. By reason of ease of implementation, cubic neighbourhood is applied to define the adjacent relationship. Then, the neighbouring voxels are sorted and any empty voxel is removed if presents in the sorted neighbouring voxels. When a set of the sorted neighbouring voxels is free from empty voxels, *n%* of the upper and lower values are removed. This removal is meant to obtain an average value which is closer to the estimated value by assuming that the estimated value tends to lie in the neighbourhood of the mid-range instead of located in the outliers.

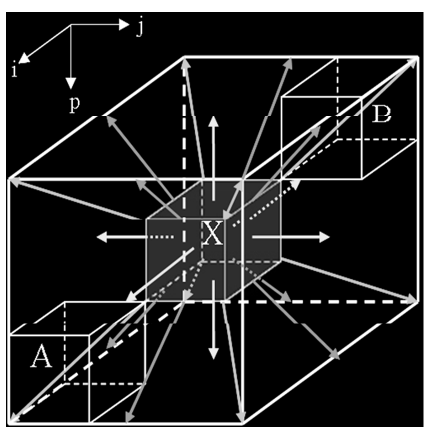

Figure. 8.3. The 26 neighbouring voxels of the empty voxel X with distance r=1

The conventional Olympic method took an average value to fill the empty voxel. However, in reality there must be variability that causes the values to lie not exactly in such average intensity. It follows that a thresholding method is used to improve the estimation result. In this regard, the average of the range width of the remaining sorted neighbouring voxels in all existing empty voxels, $\overline{R}_n$, with a factor of k, is used as a threshold to classify the values. The range width value of each empty voxel, R_n, which is calculated from the subtraction of the maximum and minimum values, is then compared to the thresholding value. The adjustment of the average and the range width values determine the approximated empty voxel values. The thresholding can be described as follows

$$x_e = \overline{x}_n - \left(\frac{R_n}{p}\right), \text{ where } \begin{array}{l} p = p_1 \ , R_n \le k.\overline{R}_n \\ p = p_2 \ , R_n > k.\overline{R}_n \end{array} \tag{3}$$

where x_e is the estimated empty voxel, $\overline{x}_n$ is the average of the remaining sorted neighbouring voxels, R_n is the range width of the remaining sorted neighbouring voxels, p is the value determined by the threshold value of $k.\overline{R}_n$. p_1 is the value of p if $R_n \le k.\overline{R}_n$., and p_2 is the value of p if $R_n > k.\overline{R}_n$.

8.5. Testing the Improved Olympic Hole Filling

We have implemented the proposed hole-filling algorithm in the 3DUS volume reconstruction described using Matlab 7.0.4. A set of 3DUS volume of the vertebra scanned with a very dense sweep and no hole was used to test the performance of the proposed method. The non-holed 3DUS volume was used to confirm the performance of the algorithm in filling the holes with the correct ones from the acquisition. The volume was cropped to $70\times70\times70$ voxels by including two areas of interest, the vertebral surface and the soft tissue parts. The artificial holes were made in certain locations to mimic the original holes in the 3DUS volume reconstruction. The test was accomplished by taking 10% removal of the upper and lower parts of the sorted neighbouring empty voxels, $k = 0.8$, $p_1 = 20$, and $p_2 = 2.5$.

The performance of the proposed Hole-filling method was measured by means of MAE. This method quantifies how close the estimated hole filled value is to the original value. To determine the quality of the proposed method, the proposed method was compared with the conventional Olympic [12], average [19], and maximum [19] method.

8.6. Experimental Results and Discussions

In Figure. 8.4a-d, we demonstrate one slice of the cropped 3DUS volume as original non-holed and hole-manipulated, and the residue after using the proposed methods respectively. The residue is subtraction between the hole-filled with the original non-holed slice. In this regard, all the images are inverted for ease of visual recognition reason. Table. 8.1 presents the quantitative results for the MAE results of the estimated hole-filled volume of the tested methods with the original hole values from the acquisition.

In this study, the ultrasound volume reconstruction of the spine is performed in two main steps, the Bin-filling and the Hole-filling. In the Bin-filling, we apply a maximum value for residing a voxel occupied by more than one pixel since it was already investigated in the previous study [12] that the maximum pixel value generates the most optimal Bin-filling in our 3DUS volume reconstruction of the spine application where the reflection of the ultrasound signal to the expected spinal features has the highest intensity than other materials in the ultrasound image (e.g; muscle, inner side of the bone, and other soft tissues). Therefore, employing the maximum value in the Bin-filling preserves the acquired spinal feature.

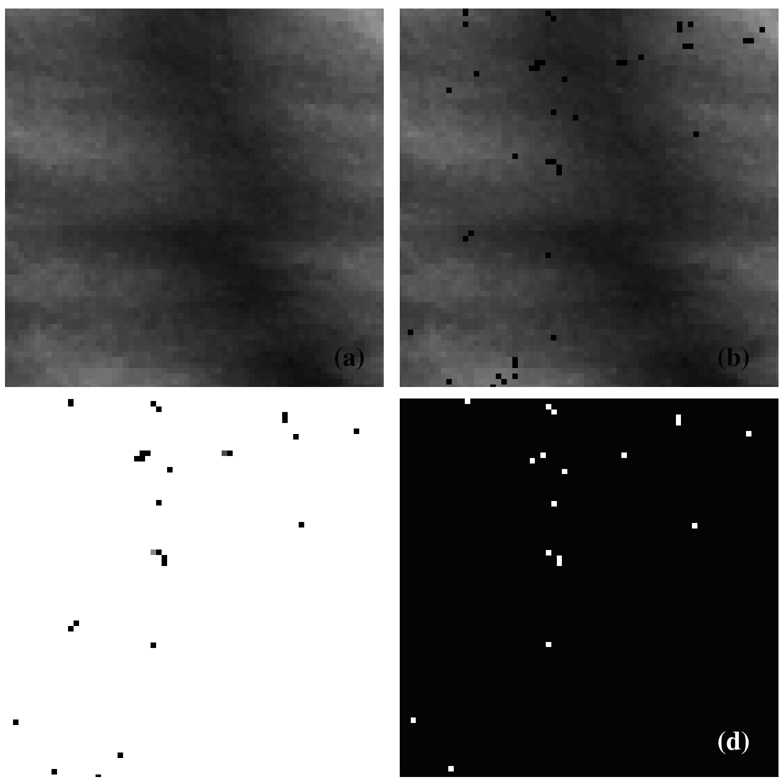

Figure. 8.4. (a) Original non-holed slice, (b) Hole-manipulated slice, (c) Residue between the original and the hole-filled slices using the conventional Olympic method, and (d) the improved Olympic method.

Table. 8.1. Mean absolute error calculation for comparison of the 4 hole-filling methods

METHODS	MAE
Improved Olympic	0.0069
Conventional Olympic	0.0219
Average	0.0070
Maximum	0.0197

In the Hole-filling, a modification of the conventional Olympic method is intended to improve the performance of the Olympic Hole-filling in estimating the value and occupying the empty voxels in the 3DUS volume reconstruction of the spine. This improved algorithm estimates the empty voxel value, not only by taking the average value of the shrinked neighbouring voxels with the cutback ratio of 10%, but also approximating the average to the actual value by adding a weighting value from the remaining range width values with a factor of $1/p$ to the average value. A threshold of the average of the range width values in all empty voxels with a factor of k is used to classify the estimated empty voxel candidates based on the range width value. If the range width value is higher than the threshold, the estimated empty voxel is assumed to lie far from the average value. On the other hand, if the range width value is lower than the threshold, the estimated empty voxel is expected to locate closer to the average value.

In our proposed improved Olympic operator, we tested with 10% removal of the upper and lower values of the sorted neighbouring empty voxels. We chose the ratio of 10% by considering that we merely applied distance with r = 1 in this study, therefore a number of empty voxels in the neighbourhood of the appointed empty voxel that we excluded from the calculation might limit the analysis. However, it is recommended to investigate the optimum distance value of r and the cutback ratio of $n\%$ to estimate the best hole value.

Furthermore, we have tested the 3DUS volume reconstruction by means of the improved Olympic Hole-filling method by varying several parameters and found that the thresholding factor of $k = 0.8$ with the weighting value of $p_1 = 20$, and $p_2 = 2.5$ produce the lowest MAE result of 0.0069 compared to other values in this method.

In addition, a comparison of the MAE calculation on several Hole-filling methods (Improved Olympic, Conventional Olympic, Average, and Maximum) shows that the improved Olympic Hole-filling method gives the lowest MAE calculations. As shown in the residue slices in Figure. 8.4c-d and the MAE results, the improved Olympic appears a significant improvement compared to the Conventional Olympic and Maximum hole-filling method. However, a slight improvement of the MAE result between the improved Olympic and the average method in this study may also indicate that the proposed method has a comparable performance as the average Hole-filling method.

8.5. Conclusions

We have presented an improvement of the conventional olympic hole-filling method in the ultrasound volume reconstruction of the spine using freehand 3DUS system.

The improved olympic hole filling method estimates the hole values by employing the conventional olympic hole filling and adding a thresholding method and adjustment of the average and the range width values in the calculation. Initial test on this algorithm shows a better empty voxel estimation among other tested methods.

References

[1] A. Fenster and D. B. Downey, "Three-dimensional ultrasound imaging," *Annu Rev Biomed Eng*, vol. 2, no. 1, pp. 457-475, 2000.

[2] O. V. Solberg, F. Lindseth, H. Torp, R. E. Blake, and T. A. Nagelhus Hernes, "Freehand 3D Ultrasound Reconstruction AlgorithmsùA Review," *Ultrasound Med Biol*, vol. 33, no. 7, pp. 991-1009, 2007.

[3] M. Brunner, A. Obruca, P. Bauer, and W. Feichtinger, "Clinical application of volume estimation based on three-dimensional ultrasonography," *Ultrasound Obst Gyn*, vol. 6, no. 5, pp. 358-361, 2003.

[4] A. Scharf, M. F. Ghazwiny, A. Steinborn, P. Baier, and C. Sohn, "Evaluation of two-dimensional versus three-dimensional ultrasound in obstetric diagnostics: a prospective study," *Fetal diagn ther*, vol. 16, no. 6, pp. 333-341, 2000.

[5] M. L. Manini, D. D. Burton, D. D. Meixner, D. J. Eckert, M. Callstrom, G. Schmit, M. El-Youssef, and M. Camilleri, "Feasibility and application of 3-dimensional ultrasound for measurement of gastric volumes in healthy adults and adolescents," *J Pediatr Gastr Nutr*, vol. 48, no. 3, pp. 287, 2009.

[6] R. Campani, O. Bottinelli, F. Calliada, and D. Coscia, "The latest in ultrasound: three-dimensional imaging. Part II," *Eur J Radiol*, vol. 27, p. S183-S187, 1998.

[7] F. Candiani, "The latest in ultrasound: three-dimensional imaging. Part 1," *Eur J Radiol*, vol. 27, p. S179-S182, 1998.

[8] A. Gee, R. Prager, G. Treece, and L. Berman, "Engineering a freehand 3D ultrasound system," *Pattern Recogn Lett*, vol. 24, no. 4-5, pp. 757-777, 2003.

[9] Q. H. Huang, Y. P. Zheng, M. H. Lu, and Z. R. Chi, "Development of a portable 3D ultrasound imaging system for musculoskeletal tissues," *Ultrasonics*, vol. 43, no. 3, pp. 153-163, 2005.

[10] S. Suzuki, T. Yamamuro, J. Shikata, K. Shimizu, and H. Iida, "Ultrasound measurement of vertebral rotation in idiopathic scoliosis," *J Bone Joint Surg Br*, vol. 71, no. 2, pp. 252-255, 1989.

[11] B. Brendel, S. Winter, A. Rick, M. Stockheim, and H. Ermert, "Registration of 3D CT and ultrasound datasets of the spine using bone structures," *Computer Aided Surg*, vol. 7, no. 3, pp. 146-155, 2002.

[12] I. K. E. Purnama, M. H. F. Wilkinson, A. G. Veldhuizen, P. M. A. van Ooijen, T. A. J. Lubbers, J. G. M. Burgerhof, T. A. Sardjono, and G. J. Verkerke, “A framework for human spine imaging using a freehand 3D ultrasound system,“ *Technol Health Care*, vol. 18, pp. 1–17, 2010.

[13] C. D. Barry, C. P. Allott, N. W. John, P. M. Mellor, P. A. Arundel, D. S. Thomson, and J. C. Waterton, "Three-dimensional freehand ultrasound: image reconstruction and volume analysis," *Ultrasound Med Biol*, vol. 23, no. 8, pp. 1209, 1997.

[14] T. R. Nelson and D. H. Pretorius, "Three-dimensional ultrasound imaging," *Ultrasound Med Biol*, vol. 24, pp. 1243-1270, 1998.

[15] P. Coupe, P. Hellier, N. Azzabou, and C. Barillot, "3D freehand ultrasound reconstruction based on probe trajectory," *Lect Notes Comput Sc*, vol. 3749, pp. 597-604, 2005.

[16] D. G. Gobbi and T. M. Peters, "Interactive intraoperative 3D ultrasound reconstruction and visualization," *Lect Notes Comput Sc*, vol. 2488, pp. 156-163, 2002.

[17] F. Hottier and A. C. Billon, *3D echography: status and perspective*, in 3D Imaging in Medicine: Algorithms, Systems, Applications, Berlin, Germany: Springer-Verlag, pp. 21-41, 1990.

[18] H. A. McCann, J. C. Sharp, T. M. Kinter, C. N. McEwan, C. Barillot, and J. F. Greenleaf, "Multidimensional ultrasonic imaging for cardiology," *Proc IEEE*, vol. 76, no. 9, pp. 1063-1073, 1988.

[19] T. R. Nelson and D. H. Pretorius, "Interactive acquisition, analysis, and visualization of sonographic volume data," *Int J Imag Syst Tech (Special Issue: Acoustical Tomography,)*, vol. 8, no. 1, pp. 26-37, 1997.

[20] R. Ohbuchi, D. Chen, and H. Fuchs, "Incremental volume reconstruction and rendering for 3-D ultrasound imaging," *Proc. SPIE*, vol. 1808, pp. 312–323, 1992.

[21] R. Rohling, A. Gee, and L. Berman, "A comparison of freehand three-dimensional ultrasound reconstruction techniques," *Med Image Anal*, vol. 3, no. 4, pp. 339-359, 1999.

[22] R. San Jose-Estepar, M. Martin-Fernandez, P. P. Caballero-Martinez, C. berola-Lopez, and J. Ruiz-Alzola, "A theoretical framework to three-dimensional ultrasound reconstruction from irregularly sampled data," *Ultrasound Med Bio*, vol. 29, no. 2, pp. 263-278, 2003.

[23] J. W. Trobaugh, D. J. Trobaugh, and W. D. Richard, "Three-dimensional imaging with stereotactic ultrasonography," *Comput Med Imaging Graph*, vol. 18, no. 5, pp. 315-323, 1994.

[24] R. S. J. Estepar, M. Martin-Fernandez, C. berola-Lopez, J. Ellsmere, R. Kikinis, and C. F. Westin, "Freehand ultrasound reconstruction based on ROI prior modeling and normalized convolution," *Lect Notes Comput Sc*, no. 2879, pp. 382-390, 2003.

[25] R. Rohling, A. Gee, and L. Berman, "Three-dimensional spatial compounding of ultrasound images," *Med Image Anal*, vol. 1, no. 3, pp. 177-193, 1997.

[26] S. Meairs, J. Beyer, and M. Hennerici, "Reconstruction and visualization of irregularly sampled three-and four-dimensional ultrasound data for cerebrovascular applications," *Ultrasound Med Biol*, vol. 26, no. 2, pp. 263-272, 2000.

[27] J. C. Russ, *The image processing handbook*, CRC press, Boca Raton, Florida , 2006.